AAPS PharmSciTech, Vol. 13, No. 2, June 2012 (© 2012)
DOI: 10.1208/s12249-012-9758-7

Research Article

Enhanced Antibacterial Effect of Ceftriaxone Sodium-Loaded Chitosan Nanoparticles Against Intracellular *Salmonella typhimurium*

Noha M. Zaki[1,2,4] and Mohamed M. Hafez[3]

Received 3 June 2011; accepted 1 February 2012; published online 23 February 2012

Abstract. The aim of the present study was to utilize chitosan (CS) nanoparticles for the intracellular delivery of the poorly cell-penetrating antibiotic, ceftriaxone sodium (CTX). *In vitro* characterization of (CTX-CS) nanoparticles was conducted leading to an optimized formula that was assessed for its biocompatibility to blood (hemolysis test) and cells (MTT assay). Progressively, confocal laser scanning microscopy (CLSM), cellular uptake (microfluorimetry), and antibacterial activity of the nanoparticles were investigated in two cell lines: Caco-2 and macrophages J774.2 pre-infected with *Salmonella typhimurium*. Results showed that the optimized formula had size 210 nm, positive zeta potential (+30 mV) and appreciable entrapment efficiency for CTX (45%) and included a biphasic release pattern. The nanoparticles were biocompatible and were internalized by cells as verified by CLSM whereas microfluorimetry indicated substantial cellular uptake. Moreover, the CTX–chitosan nanoparticles showed a significant reduction in the count of intracellular *S. typhimurium* in Caco-2 and macrophages J774.2. This reduction was significantly higher than that obtained in case of placebo nanoparticles, CTX, and CTX–chitosan solutions and might be attributed to enhanced endocytic uptake of the nanoaprticles and antibacterial effect of the chitosan polymer. In conclusion, the results provide evidence for the potential use of chitosan nanoparticles to enhance the intracellular delivery and antibacterial effect of CTX in enterocytes and macrophages.

KEY WORDS: ceftriaxone sodium; chitosan nanoparticles; enterocytes; intracellular delivery; macrophages.

INTRODUCTION

The purpose of this study was to explore the possible improvement of antimicrobial treatment by its incorporation into chitosan-based nanoparticles. Limited cellular penetration reduces the effectiveness of many antimicrobial treatments; this is true in the case of the third-generation cephalosporin, ceftriaxone sodium (CTX). While CTX has demonstrated activity against most *Salmonella* spp. *in vitro* (1–6), it was demonstrated to be ineffective in killing intracellular pathogens (7–9). Moreover, it showed clinical failure in treating salmonellosis (10). The poor cellular penetration of the antibiotic was attributed to its high molecular weight (661.6) as well as its hydrophilicity (log P −0.6) (11–16). Efforts have been made to increase its oral absorption. One attempt aimed at increasing its functional lipophilicity through the formation of ion pairs by coupling with positively charged bile acids (12,17). Another aimed at using absorption enhancers for increasing its membrane permeability (18). One strategy to improve cellular access is to incorporate the antibiotic into a nanoparticulate system that would be ingested by phagocytic cells of the mononuclear phagocytic system (MPS), (19–21). In addition to the selective delivery to phagocytes, the ingestion of such vehicles may involve macrophage activation, and increasing the immune response of the host (22). Other advantages for antibiotic nanoparticles include enhancement of oral absorption, promotion of intracellular delivery (23–26), and improvement of the antibacterial effect (27–29). Nanoparticulate systems that increase the selectivity of antibiotics in phagocytic cells have been reviewed elsewhere (19), most of which were based on biodegradable poly(lactide-co-glycolide polymer (25,28, 30,31). Chitosan nanoparticles were recently used as a carrier for aminoglycosides (32), but the study has not explored the intracellular delivery capabilities. To the best of our knowledge, the utility of chitosan nanoparticles for intracellular antibiotic delivery has not yet been reported and therefore is highly warranted.

The results from previous studies on the antibacterial properties and the non-specific endocytic cellular uptake of chitosan nanoparticles (33) led us to design chitosan–tripolyphosphate (CS/TPP) nanoparticles loaded with CTX against

[1] Department of Pharmaceutics and Pharmaceutical Technology, College of Pharmacy, Taif University, Taif, Kingdom of Saudi Arabia.
[2] Department of Pharmaceutics and Pharmaceutical Technology, Faculty of Pharmacy, Ain Shams University, Monazamet El Wehda El Afrikia St, El Abbassia, Cairo, Egypt.
[3] Department of Microbiology and Immunology, College of Pharmacy, Taif University, Taif, Kingdom of Saudi Arabia.
[4] To whom correspondence should be addressed. (e-mail: anm1998@lycos.com)

Salmonella typhimurium as a model Gram-negative intracellular pathogen. The capabilities to shuttle the poorly permeable antibiotic to the intracellular milieu as well as the antibacterial enhancement effect mediated and/or augmented by chitosan nanoparticles will be tested in two cell lines namely: Caco-2 as a model of enterocytes where the *Salmonella* reside after food poisoning and macrophages J774.2 cells where pathogens survive and replicate inside the MPS.

EXPERIMENTAL

Materials

Pentasodium triphosphate (Fluka), 1 N hydrochloric acid, 1 N sodium hydroxide, and dimethyl sulfoxide (DMSO) were purchased (Aldrich, UK); ceftriaxone sodium (CTX), gentamicin sulfate, dimethylthiazole tetrazolioum bromide (MTT) and fluorescein isothiocyanate (FITC) from Sigma (UK) and glacial acetic acid (VWR BDH Chemicals) were used as received. The 10 mM phosphate buffered saline (PBS) was prepared from appropriate tablets (Oxoid, Basingtoke, UK). Chitosan (Aldrich) was used after purification (degree of deacetylation and average molecular weight were 85% and 492×10^3 g/mol, respectively).

The QuantiPro BCA assay kit was supplied from Sigma; a solution of 1.0 mg/ml bovine serum albumin (Sigma) in 0.15 M NaCl was used as a standard.

Bacteria

Clinical isolates of *S. typhimurium* were kindly provided from Faculty of Life Sciences, University of Manchester. The bacteria were cultured by incubation at 37°C in Luria–Bertani broth overnight for 18 h. All bacteria were stored on plates at 4°C or in frozen stock at −70°C.

Cell Culture

Caco-2 and macrophages J774.2 cells (ECACC, UK) were maintained as, respectively adherent and semi-adherent cell cultures at 37°C in a humidified atmosphere (5% CO_2) in Dulbecco modified Eagle's minimal essential medium (DMEM, 25 mM glucose) supplemented with 2 mM glutamine (Gibco) and 10% heat-inactivated fetal calf serum (FCS) (Invitrogen, UK). Antibiotic solution composed of 100 IU/ml penicillin and 100 IU/ml streptomycin (Gibco) was added to the culture medium during cell maintenance and excluded in bacterial infection experiments. For monolayer formation, Caco-2 were detached using trypsin–EDTA (Invitrogen, UK) consisting of 2.5% (*w/v*) of trypsin and 0.2% (*w/v*) EDTA in PBS while macrophages J774.2 cells were detached mechanically by scraping. The cells were suspended in DMEM containing FCS to a count of 10^5 living cells/ml as determined by trypan blue exclusion stain and a hemocytometer. For cytotoxicity, cellular uptake, and antibacterial assessment experiments, aliquots of the cells were seeded in 96-well plates and incubated till confluency. For confocal microscopy, cells were seeded on coverslips in a six-well plate.

Methods

Preparation of FITC-Labeled Chitosan

Chitosan labeling was performed as previously described (34), with slight modification. Briefly, purified chitosan was dissolved in 0.10 M acetic acid to a concentration 5.6 mg/ml; the pH was adjusted to 4 with 1 N sodium hydroxide. FITC dissolved in DMSO (5 mg/ml) was slowly added to the chitosan solution. The reaction was left stirring for 12 h. The pH was adjusted to 4 using 1 N HCl until a clear solution was achieved; the mixture was purified by ultra-filtration and then freeze-dried.

Preparation of Nanoparticles

The chitosan–TPP nanoparticles were prepared via TPP ionic crosslinking and coacervation method as previously mentioned (35). Briefly, chitosan (1 mg/ml) was dissolved in 5 mM HCl solution and the pH adjusted to 4 or 5 using 1 N NaOH. Then, TPP solution (1 mg/ml; adjusted to either pH 4, 5, or 8) was added to the chitosan solution, and the mixture was stirred (750 rpm) for 30 min at room temperature. The two solutions were mixed at different pH combinations namely 4/4, 5/5, and 4/8 for CS/TPP, respectively. The nanoparticles were formed at various chitosan to TPP weight ratios of 5:1, 7:1, 9:1, 11:1, and 13:1 and the resulting mixtures were observed to be either clear, opalescent, or consisting of aggregates. The conditions for the formation of opalescent nanoparticles were further assessed. Drug-loaded nanoparticles were prepared by the incorporation method (36) only at pH 5/5 for CS/TPP, in which different amounts of CTX were dissolved in the TPP solution at pH 5, which was then mixed with the CS or FITC-labeled CS solution at pH 5, and the procedure was repeated as mentioned above. After nanoparticle formation, the pH was raised to pH 6 by the addition of small volumes of 0.1 NNaOH. The formulations were then freeze-dried in the presence of 0.1% sucrose used as a cryoprotectant (Heto Drywinner, Thermo Scientific, USA) for 24 h at a pressure of 0.05 mmHg. As a control, CTX–CS solution was prepared with same concentrations of CTX and CS, but without the addition of TPP to avoid the formation of nanoparticles.

Physicochemical Characterization of Chitosan Nanoparticles

The freshly prepared nanoparticles were subjected for measurement of particle size, zeta potential, and size distribution (polydispersity index (PDI)) without sample dilution or any salt addition. Dynamic light scattering and zeta potential measurements were performed in triplicate on a Zetasizer Nanoseries ZEN3600 (Malvern Instruments, UK) equipped with a solid state He–Ne laser (λ=633 nm). All the samples were analyzed at an angle of 114° and a temperature of 25°C.

Encapsulation Efficiency of Antibiotic in Nanoparticles

The encapsulation efficiency and loading capacity of nanoparticles were determined after purification of the nanoparticles by centrifugation at 16,000×*g* for 30 min at

15°C on a glucose bed (35%, 50 μL). The amount of free CTX in the supernatant was measured spectrophotometrically at 272 nm using a preconstructed calibration curve made using serial concentrations of CTX (0.005–0.014 mg/ml) in distilled water adjusted to pH 6 ($y = 50.98x - 0.079$; $R^2 = 0.975$).

The encapsulation efficiency (EE%) and the loading capacity (LC%) of the nanoparticles were calculated as follows:

$$\mathrm{EE}(\%) = \frac{\text{Total ceftriaxone Na} - \text{free ceftriaxone Na}}{\text{Total ceftriaxone Na}} \times 100 \quad (1)$$

$$\mathrm{LC}(\%) = \frac{\text{Total ceftriaxone NA} - \text{free ceftriaxone Na}}{\text{Nanoparticles weight}} \times 100 \quad (2)$$

All measurements were done in triplicates.

In Vitro Release of CTX from the Nanoparticles

In vitro release of CTX from chitosan nanoparticles was determined as previously described (37). An amount of freeze-dried nanoparticles equivalent to 5 mg CTX was re-dispersed in 5 mL 0.15 M PBS solution (pH 6) and placed in a dialysis membrane bag with a molecular cut-off of 5 kDa, tied, and then placed into 50 ml of PBS solution pH 7.4. The entire system was kept at 37°C with continuous magnetic stirring. At appropriate time intervals, 3 ml of the release medium was removed, and replaced by 3 ml fresh PBS solution. The amount of CTX in the release medium was evaluated spectrophotometrically after appropriate dilution. All measurements were done in triplicates.

Freeze-Drying and Redispersibility of Colloids

To study the physical stability of the colloid after lyophilization and redispersion, the optimized formulations were freeze-dried in presence of sucrose (0.1% *w/v*) as a cryoprotectant for 48 h at a 0.05 mmHg pressure. Once per month, freeze-dried samples stored at room temperature (on a lab bench at 25°C) were redispersed by vortex mixing with 10 ml of ultrapure water, and the particle size, PDI, zeta potential, and *in vitro* drug release were re-assessed.

Biocompatibility Studies

Blood Compatibility. Blood compatibility was studied using hemolysis experiments as previously reported (38) using human blood. The experimental procedures conformed to the ethical guidelines of the Experiments and Advanced Pharmaceutical Research Unit, Ain Shams University, on the use of the human blood. Briefly, the blood was centrifuged at 3,000 rpm for 5 min, and the obtained erythrocyte pellets were washed four times with normal saline. Finally, after repeated washing and centrifugation, an appropriate amount of PBS was added to the erythrocyte pellets to obtain a 10% erythrocyte standard dispersion. Subsequently, 1.75 ml of distilled water, PBS, or nanoparticles dispersion in PBS was mixed with 0.25 ml of 10% erythrocyte standard solution. The mixture was incubated for 20 min at 37°C and then centrifuged for 5 min at 2,000 rpm. The absorbance of the supernatant was measured at 543 nm. The absorbances of the supernatant when using distilled water and PBS were assumed to be 100% and 0%, respectively.

Compatibility to Cells. The three-step protocol for testing the cell compatibility of high concentrations of nanoparticles was adopted as per our previous publication (39). Briefly, nanoparticles were first purified by ultra-filtration (500 kDa molecular weight cut-off polyethersulphone membranes) and freeze-dried in the presence of 0.1% sucrose as a cryoprotectant to avoid lumping upon redispersion. The colloids were dispersed in the least possible volume of water and dialyzed against water to remove sucrose. The highly concentrated colloidal dispersion prepared herein served as stock from which appropriate dilutions were made at the time of the experiment. Eventually, dispersions of nanoparticles to be tested on the cells were obtained by mixing one part of five times more concentrated culture medium and four parts of the different nanoparticle dispersions on a vortex mixer. Isotonicity was checked with an osmometer (OSMOMAT 010, Gonotec, UK) and adjusted if necessary (300 ± 10 mOsm/kg) with mannitol before incubation with cells. Caco-2 cells were trypsinized while macrophages J774.2 were split by mechanical scraping. Cell suspensions were diluted with culture medium to a count of 1×10^5 cells/ml and seeded in 96-well micro-titer plate at density of 10,000 cells/well. At the time of each experiment, the culture medium was removed and replaced with 100 μl of the different nanoparticle dispersions (different concentrations) or of the control. After 24 h incubation at 37°C in a humid atmosphere with 5% CO_2, the colloidal dispersion was removed by gentle aspiration and the cells were rinsed three times with pre-warmed pH 7.4 PBS. Then, 100 μl of 3-[4,5-dimethylthiazol-2-yl]-3,5-diphenyl tetrazolium bromide dye (MTT reagent) (0.5 mg/ml in DMEM) was added to each well, and the plates were incubated for 4 h after which the stain was removed; 100 μl of sterile DMSO was added to each well, and the plates were shaken for 5 min to solubilize the crystals (40). Finally, the absorbance (A) was measured at 550 nm in a micro-titer plate reader (TECAN Safire, Tecan Austria GmbH, Grödig, Austria). The cell viability was calculated using the following equation:

$$\text{Cell viability}\,(\%) = A_{\text{test}}/A_{\text{control}} \times 100$$

Where A_{test} is the absorbance of the cells incubated with the different nanoparticles dispersions and A_{control} is the absorbance of the cells incubated with the culture medium only (negative control). IC_{50}, the drug concentration at which reduction of 50% cell viability occurs in comparison with that of the control sample, is calculated by the curve fitting of the cell viability data (41,42).

Cellular Uptake Studies

Confocal Microscopy. The cellular uptake using confocal laser scanning microscopy was performed as per our previous publication (39). Briefly, Caco-2 cells and macrophages J774.2

were seeded on sterile poly-L-lysine-coated coverslips placed in six-well plates and placed in the incubator at 37°C to allow cell attachment. To each well, 250 μl of nanoparticle dispersion was added, and the plates were incubated for 30 min in a humid atmosphere at 37°C in a CO_2 incubator. Immediately after removal of the colloidal dispersion by gentle aspiration, 1 ml trypan blue solution was incubated with the cells for 1 min after which the cells were rinsed at least four times with pre-warmed PBS pH 7.4. Cell fixation and permeabilization was achieved by dipping in 4% formaldehyde solution for 20 min at room temperature followed by 0.05% Triton X-100 in PBS for 5 min. After rinsing with PBS, the cells were incubated for 3 min with 200 nM 4',6-diamidino-2-phenylindole (DAPI) solution in PBS for nuclear staining followed by rinsing. The coverslips were carefully inverted onto a drop of mounting liquid on a microscopic slide and stored in the dark at 4°C. For visualization using confocal microscopy, excitation at 485 nm induces the FITC fluorescence (green emission) of the labeled nanoparticles while excitation at 358 nm induces DAPI fluorescence (blue emission). For further image processing, ImageJ® Software was used.

Microfluorimetry Assay. For quantitative study, Caco-2 cells and macrophages J774.2 were seeded into 96-well plates (black wall with transparent bottom, Costar, IL, USA) at 1.3×10^4 cell/well, and after the cells reached 80% confluence, the medium was changed with that containing FITC-labeled nanoparticles of varying concentrations 0.002–0.05 mg/ml. After 30 min incubation, the suspension was removed and the wells were washed with 100 μl of PBS to eliminate traces of nanoparticles left in the wells. Fifty microliters of 0.5% Triton X-100 in 0.2 N NaOH was added to the sample wells at room temperature to lyse the cells. The amount of fluorescence of the cell lysate in each well was then measured using a fluorescence plate reader (TECAN Safire, Tecan Austria GmbH, Grödig, Austria) with excitation wavelength at 485 nm and emission wavelength at 520 nm for FITC. Cell-bound and internalized nanoparticles are quantified by making use of a calibration curve obtained with FITC-labeled nanoparticles in a cell lysate solution (10^6 untreated cells dissolved in 1 ml of the Triton X-100 solution). The protein content of the cell lysate in each well was determined using the QuantiPro micro BCA protein assay kit (Sigma, MO, USA). Uptake was expressed as the amount (micrograms) of nanoparticles associated with unit weight (milligrams) of cellular protein. To determine the kinetics of nanoparticles uptake by cells, different incubation times 0, 10, 15, 30, 45, 60, 90, and 120 min were used. The experiments were repeated at 4°C to determine whether nanoparticle uptake by cells is energy-dependent.

Intracellular Antibacterial Effect. Placebo nanoparticles, CTX solution, CTX-CS solution, as well as CTX-CS nanoparticle formulation (CTX, 1 mg/ml; CS, 1 mg/mL; TPP, 1 mg/mL at CS/TPP ratio=9:1, and pH 5/5) were tested for their ability to kill intracellular pathogens infecting Caco-2cells or macrophages J774.2 cells in a previously validated *in vitro* cell infection model (43). The bacteria used in these experiments were wild-type *S. typhimurium* SL1344 strain. Before cell infection, the bacterial suspension was washed once in PBS and then adjusted to an optical density of 0.1 at 600 nm equivalent to 10^8 colony forming unit (CFU per milliliter). For invasion of cells with *Salmonella*, 0.5-ml aliquot of bacterial suspension was added to each well-containing monolayer at multiplicity of infection of 100 and incubated for 90 min at 37°C in 5% CO_2. After infection, the cells were washed three times with PBS and were then treated with gentamicin sulfate (200 μg/ml) for 1 h (conditions under which gentamicin sulfate is membrane-impermeative and almost exclusively kills extracellular bacteria). The cells were again washed five times with PBS. To test for the killing of intracellular bacteria, the cells were incubated with CTX solution, CTX-CS solution, CTX-CS nanoparticles, or placebo nanoparticles for different intervals—15, 30, 60, 90, and 120 min after which the cells were washed three times with PBS and then lysed with 0.5% Triton X-100 in 0.2 N sodium hydroxide in water. Dilutions of the lysates were grown overnight at 37°C on Luria–Bertani plates, and the numbers of CFU of *S. typhimurium* were counted according to the viable count technique. The concentration of nanoparticles used in the antibacterial study was 0.12 mg/ml equivalent to 50 μg/ml ceftriaxone sodium (this concentration is safe to the cells for 4 h as tested by cytotoxicity study using MTT assay).

Statistical Analysis

All tests were conducted in triplicate, and the results were expressed as the mean±standard deviation. Statistical analysis of the data was performed using one-way analysis of variance (ANOVA) followed by the Bonferroni test for multiple comparison at $P<0.05$ using Instat-ANOVA software.

RESULTS

Physicochemical Characterizations of Nanoparticles

Results revealed that unmedicated CS/TPP nanoparticles had a size range from 91 to 288 nm and a positive zeta potential ranging from 18 to 46 mV (Table I). The CS/TPP weight ratio as well as pH of both solutions affected particle size and zeta potential where an increase in nanoparticle size and zeta potential was observed with increase in the CS/TPP weight ratio.

The colloidal stability of formulations prepared at CS/TPP mass ratio 9/1 with pH values 5/5 for both solutions was maintained after 4 months storage in refrigerator (Table I). Particle aggregation, appearance of fines, or increase in polydispersity was not observed, hence, this formulation was selected for CTX loading in further studies.

Incorporation of CTX affected the size and zeta potential of the optimized nanoparticles as shown in Table II. The particle sizes of CTX-loaded nanoparticles significantly increased while the zeta potentials was decreased significantly as the concentration of CTX increased from 0.1 to 1.5 mg/ml.

Concerning the entrapment of the antibiotic in the nanoparticles, results showed that the encapsulation efficiency and loading capacity of the nanoparticles were affected by the initial CTX concentration in the TPP solution. The increase of CTX concentration led to a decrease of encapsulation efficiency and an enhancement of loading capacity. Nevertheless, CTX was entrapped in the matrix of nanoparticles to an

Table I. Particle Size, Polydispersity Index, and Zeta Potential of Plain Chitosan Nanoparticles

pH (CS/TPP)	CS/TPP weight ratio	Average particle size (nm)		Polydispersity (PDI)		Zeta potential (mV)
		Fresh	Stored	Fresh	Stored	
4/4	5/1	91.3 (1.3)	128 (2.2)	0.362	0.44	+23.3 (1.2)
	7/1	139.3 (0.6)	159 (1.6)	0.276	0.56	+36.2 (1.1)
	9/1	156.5 (2.3)	184 (2.7)	0.283	0.46	+35.9 (0.8)
	11/1	154 (1.4)	220.5 (3.1)	0.241	0.55	+37.6 (0.3)
	13/1	152.1 (1.5)	280.7 (1.9)	0.219	0.34	+39.6 (0.4)
5/5	5/1	171.8 (2.3)	178.2 (1.6)	0.169	0.22	+18.5 (1.2)
	7/1	194.9 (2.4)	198.3 (1.5)	0.227	0.23	+25.2 (2.1)
	9/1	200 (1.7)	203.3 (1.8)	0.271	0.25	+36.5 (1.8)
	11/1	204.8 (0.9)	205.1 (1.3)	0.267	0.28	+36.2 (1.88)
	13/1	239.8 (1.6)	236 (1.2)	0.4	0.41	+45.1 (1.4)
4/8	5/1	185.6 (2.2)	238 (2.4)	0.196	0.47	+33.7 (2.3)
	7/1	222.4 (1.1)	201 (1.3)	0.276	0.55	+39.4 (2.4)
	9/1	230.3 (1.3)	282.4 (2.4)	0.25	0.67	+44.2 (1.9)
	11/1	288.4 (0.5)	384 (2.8)	0.303	0.45	+41.5 (1.7)
	13/1	240.1 (0. 3)	329.3 (3.8)	0.282	0.33	+46.3 (2.1)

CS/TPP chitosan/tripolyphosphate, *PDI* polydispersity index
Chitosan concentration=1 mg/ml, TPP concentration=1 mg/ml

appreciable extent (44.7–50.3%). This might be due to binding of carboxylate group of CTX by electrostatic interaction to positively charged amino group on chitosan molecules. In presence of CTX, chitosan was still able to gel spontaneously on contact with the polyanion TPP by the formation of inter- and intramolecular crosslinkage.

In Vitro Release of CTX from Nanoparticles

The release profile of the antibiotic from a simple solution as well as from the developed nanoparticles is illustrated in Fig. 1. All the CTX in solution was released rapidly from the dialysis bag within the first 1 h. On the other hand, at all CTX-loading concentrations, nanoparticles showed a biphasic pattern with an initial burst drug release followed by a more sustained release. The CTX release was dependent on the initial concentration of the antibiotic used for encapsulation such that a greater release was achieved from nanoparticles with CTX loading at higher concentration. At 1 mg/ml CTX loading, 23% of the drug was released within the first hour followed by a slow and gradual release with 73% drug release in 96 h.

Biocompatibility Study

Nanoparticle compatibility to red blood cells (RBCs), Caco-2, and J774.2 cells was studied taking distilled water and PBS as 100% and 0% hemolysis, respectively. Results revealed that CTX-CS nanoparticles exhibited a low hemolytic percent (15%) as compared with CS solution which exhibited 50% hemolysis (Fig. 2a). This indicated that hemolysis is substantially reduced for colloid dispersion of chitosan. Regarding cell-compatibility, results revealed no significant cytotoxic effect compared with control untreated cells, i.e., almost 100% cell viability after 2 and 4 h-incubation of nanoparticles with cells at doses up to 1.8 mg/ml (results not shown). At more drastic conditions (24-h incubation), results showed that Caco-2 and J774.2 cell viability decreased in a concentration-dependent manner, such that a significant cytotoxic effect was observed at nanoparticle concentrations above 0.72 mg/ml in the case of macrophages and 1.8 mg/ml in case of Caco-2 (Fig. 2b). It is obvious that the cytotoxicity of CTX–CS nanoparticles was higher on macrophages J774.2 than on Caco-2 cell line. On the other hand, no significant drop in cell viability was observed at 4°C at all concentrations of nanoparticles tested (results not shown).

Cellular Uptake

In order to study cellular uptake of nanoparticles, the use of fluorescently or radioactively labeled nanoparticles is the most common experimental method. Fluorescent labelling makes cellular uptake of nanoparticles readily detectable by confocal laser scanning microscopy. The extent

Table II. Encapsulation Efficiency, Loading Capacity, Particle Size, Polydispersity Index, and Zeta Potential of CTX-Loaded Chitosan Nanoparticles

CTX (mg/ml)	EE (%)	LC (%)	Particle size (nm)	Polydispersity (PDI)	Zeta potential (mV)
0.1	50.3 (2.4)	25.8 (1.6)	202 (1.5)	0.21	+35.3 (1.8)
0.5	47.3 (1.8)	41.8 (2.1)	208 (0.6)	0.18	+32.5 (1.7)
1	45.5 (0.8)	46.5 (1.8)	210 (0.8)	0.25	+30.7 (1.9)
2	44.7 (1.5)	52 (2.8)	221 (1.1)	0.22	+28.5 (1.6)

EE encapsulation efficiency, *LC* loading capacity, *PDI* polydispersity index, *CTX* ceftriaxone sodium
Chitosan concentration=1 mg/ml, TPP concentration=1 mg/ml, CS/TPP ratio=9/1, pH (CS/TPP) 5/5

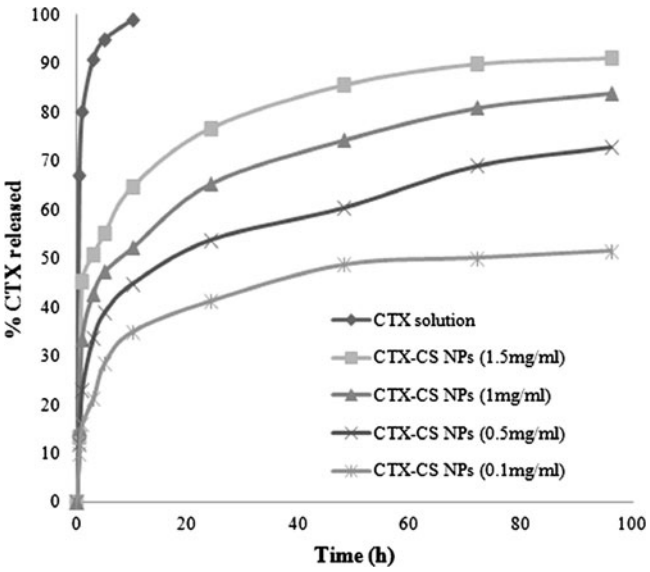

Fig. 1. *In vitro* release profiles of CTX from nanoparticle formulations at different CTX initial loading in PBS pH 6 (CS, 1 mg/mL; TPP, 1 mg/mL at CS/TPP ratio=9:1)

of particle uptake can then be determined by flow cytometry, microfluorimetry, or quantitative extraction of the markers from the cells. The Caco-2 monolayer model is an established *in vitro* tool to evaluate the intestinal uptake of drugs and/or delivery systems and inhabited by non-typhoid *Salmonella* at early stage of infection. Moreover, macrophages J774.2 were selected as a model of phagocytic cells where typhoid *Salmonella* species reside.

Figure 3a, b shows confocal microscopic images of FITC-labeled CTX-loaded CS nanoparticles incubated with Caco-2 and J774.2 cells, respectively. At 30 min post-incubation of nanoparticles with the cells, a strong green fluorescence could be seen underneath the cell membrane as well as in the cytoplasm in both Caco-2 cells and in J774.2. The extracellular and surface-associated fluorescence due to un-internalized nanoparticles was quenched by non-membrane-permeable probe: trypan blue. As such, all fluorescent signals detected were due to intracellular nanoparticles. These results indicate that CTX–CS nanoparticles were rapidly and efficiently taken up and internalized in Caco-2 and in J774.2 cells.

Cellular uptake of nanoparticles was quantified by microfluorimetric analysis. The results showed that, at 37°C, the uptake was time-, concentration-, and cell line-dependent. The kinetics of binding/uptake was very rapid and started as early as 5 min in both cell lines. The uptake followed a biphasic pattern with linear increase with time till 40 min followed by a plateau till 120 min (Fig. 4a). On the other hand, little cellular uptake was observed when experiments were performed at 4°C confirming the energy-dependent endocytic nature of the uptake of chitosan nanoparticles.

Concerning the effect of nanoparticle concentration, Fig. 4b shows that, at 60 min post-incubation of cells with nanoparticles, the uptake increased as the loading concentration (dose) of nanoparticles increased. There was a sixfold increase from 11.6 to 71.8 μg/mg in Caco-2 cells and eightfold increase from 12.6 to 94.6 μg/mg in J774.2 when the dose was increased from 0.002 to 0.05 mg/ml in both cell lines. The uptake process was saturable in both cell lines, but the levelling-off occurred at a lower concentration (0.02 mg/ml) in Caco-2 cells.

Intracellular Antibacterial Effect of CTX–CS Nanoparticles

To determine the efficacy of the nanoparticles formulation against intracellular pathogens, an *in vitro* cell-based assay was adopted. Figure 5 illustrates the antibacterial activity of 0.12 mg/ml CTX nanoparticles (proved to be non-cytotoxic in cell-compatibility test) incubated for 2 h with Caco-2 and J774.2 cells pre-infected with *S. typhimurium.* It is clear that the highest mean percent reduction in bacterial count (99% in both cell lines) was achieved in case of CTX nanoparticles. On the other hand, the mean percent reduction in bacterial counts in case of CTX solution was 33% and 49% in Caco-2 and J774.2, respectively, while the same parameter was 53% and 72% in case of CTX–CS solution for both cell line, respectively. Interestingly, plain CS nanoparticles demonstrated a small but significant antibacterial effect where the mean percent reduction in bacterial count scored 16% and 21% in Caco-2 cells and J774.2, respectively.

DISCUSSION

CTX is classified as a class III drug according to the biopharmaceutical classification system, with good aqueous solubility and poor intestinal permeability. The poor cellular penetration is attributed to its high molecular weight (661.6), high hydrophilicity (log P −0.6) and low active transport by the H+/peptide transporter PEPT1 (44). Previous studies have reported poor intestinal absorption due to efflux system for many β-lactams but not ceftriaxone. The presence of a free alpha-amino group in the molecule is an important factor for reducing an affinity with the efflux system (45–47). Our study focused on the intracellular delivery of CTX taking *S. typhimurium* as a model intracellular pathogen. The likely sites of multiplication of *Salmonella* spp. include enterocytes and phagocytes, the latter also serving as a reservoir in recurrent infections, hence, Caco-2 and macrophages J774.2 could represent the above two sites. Chitosan nanoparticles developed herein were prepared spontaneously under very mild conditions that are adaptable to aseptic manufacturing. To allow efficient cell interaction and promote intracellular delivery of CS nanoparticulate system, a high positive zeta potential is needed (48). Previous studies highlighted the importance of excess positive charge on chitosan for exerting an antibacterial effect (43–45). Another positive feature is the potential antibacterial and antityphoid effect of chitosan where it acts by disrupting the barrier properties of the outer membrane of Gram-negative bacteria (49,50). Building on this, the CS nanoparticles were engineered herein as small particles (~250 nm) with high positive charge (zeta potential>+30 mV) to maximize colloidal stability and cellular binding/internalization. As the chitosan is always found in excess, the CS/TPP mass ratio is inversely related to the cross-link density of the material but is directly related to zeta potential of the formed nanoparticles. The pH affected the ionization of both components and hence the degree of interaction between the polyelectrolytes. Smaller nanoparticle size and lower positive zeta potential were achieved at low pH couples suggesting little ionization

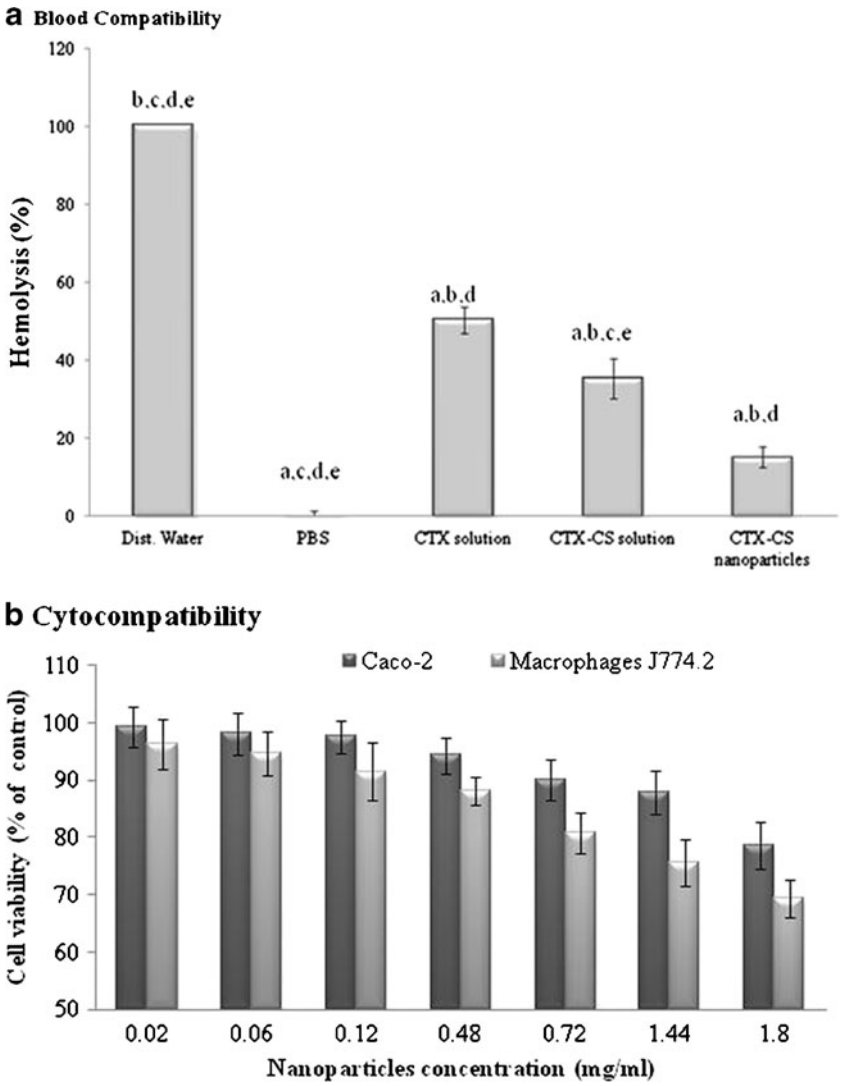

Fig. 2. Biocompatibility study of CTX–CS nanoparticles. **a** Blood compatibility (hemolytic assay) after 20 min treatment of RBCs with different CTX–CS formulations at 37°C. **a**,**b**, **c**, **d**, or **e** Significantly different from dist. water, PBS, CTX solution, CTX–CS solution, or CTX–CS nanoparticles, respectively, at $P<0.05$ using one-way ANOVA followed by Bonferroni test for multiple comparisons. **b** Cytocompatibility (MTT assay) of Caco-2 and macrophages J774.2 cells after 24-h treatment with different concentrations of CTX–CS nanoparticles at 37°C. Both cell lines demonstrated 100% viability after 2 and 4 h incubation with CTX–CS nanoparticles. The formula tested (CS, 1 mg/mL; TPP, 1 mg/mL at CS/TPP ratio=9:1 and pH 5/5)

and lower polyelectrolytes interaction. Appreciable CTX loading into the nanoparticles was achieved (46%) presumably due to electrostatic binding of the carboxylate moiety of CTX to CS nanoparticles matrix and surface. Previous studies have reported the substantial incorporation of acidic drugs (51) and negatively charged actives into positively charged CS nanoparticles (52,53). We have adjusted the pH to 6 after nanoparticle formation to favor adsorption of negatively charged CTX to positively charged nanoparticle surface; CTX would then exist in bulk of matrix as well as on the surface. The nanoparticles displayed a biphasic release pattern with an initial burst of surface-bound CTX (23% in 1 h) which was then followed by sustained antibiotic release from the bulk of nanoparticles. This release pattern could be attributed to the electrostatic interaction between the negatively charged drug (at the equilibrium pH 6) and the positively charged CS molecules. The mechanism of drug release from CS nanoparticles could be attributed to desorption from the external particle surface as well as diffusion through the porous swollen matrix (54). Erosion of the biopolymeric network with a consequent release of proteins and nucleic acids has been reported from CS nanoparticles (55), however, this may not apply herein due to its relatively low molecular weight of CTX (661.6) compared with these macromolecules. This release profile might be beneficial for the efficient treatment of intracellular infections, where a high initial dose of the surface-adsorbed antibiotic should be delivered immediately inside the cell and be followed by more sustained antibiotic release to minimize relapses.

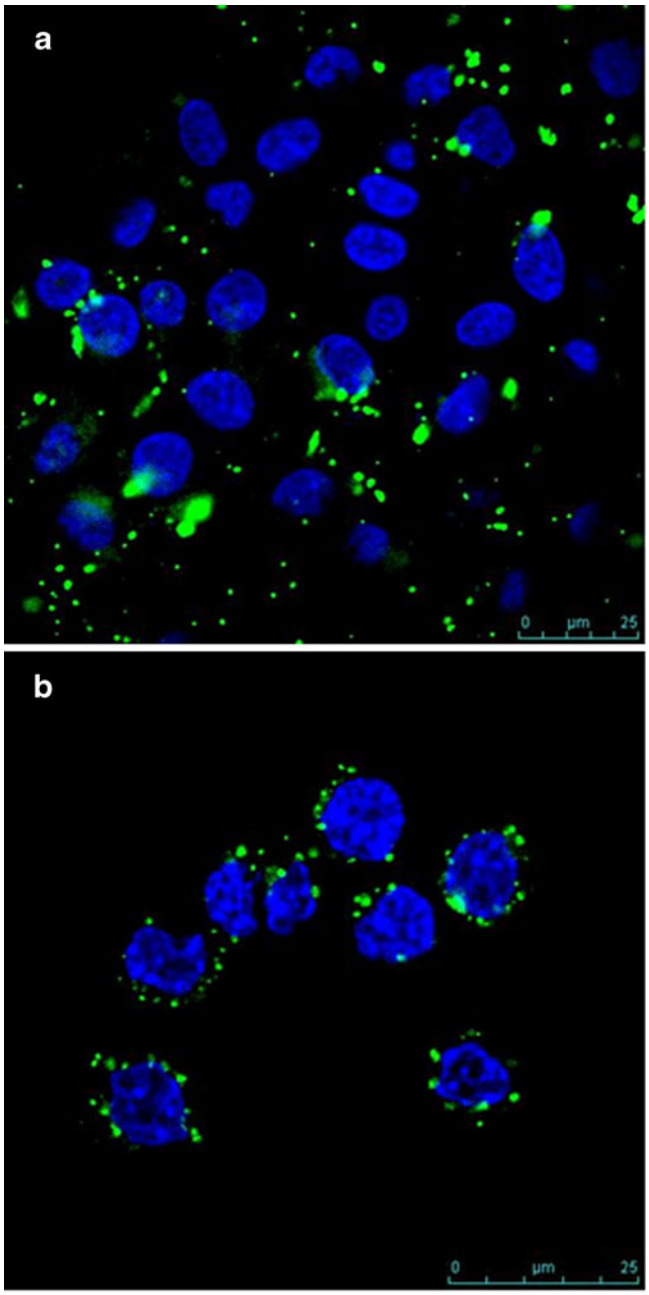

Fig. 3. Confocal images of **a** Caco-2 cell monolayers and (**b**) macrophages J774.2 coincubated for 30 min with FITC-labeled chitosan nanoparticles (*green*) followed by nucleus staining with DAPI (*blue*). The extracellular fluorescence was quenched by using trypan blue as a non-membrane-permeable probe to obtain a univocal data of intracellular fluorescence emitted by the engulfed particles. The formula tested (CS, 1 mg/mL; TPP, 1 mg/mL at CS/TPP ratio=9:1 and pH 5/5)

Biocompatibility, a key issue in the application of nanoparticles, was investigated by blood and cell compatibility study (39). A low hemolytic effect (15%) of the CS nanoparticles indicated their safety compared with CS solution (50% hemolysis). Moreover, results demonstrated a 100% cell viability at 2 and 4 h (time for antibacterial study) at doses up to 1.8 mg/ml nanoparticles over the cells as well as >70% cell viability at more drastic conditions (24 h; dose 1.8 mg/ml). These findings corroborated those previously reported (33,41,56). The cell compatibility of nanoparticles at 0.12 mg/ml (dose used in antibacterial studies) demonstrated herein would exclude the cell release of bacteria and/or extracellular killing of *S. typhimurium.*

Confocal microscopy studies verified intracellular localization of fluorescently labeled CTX–CS nanoparticles after quenching the extracellular and membrane-bound nanoparticles with trypan blue as a non-membrane-permeable probe to obtain a univocal data of intracellular fluorescence emitted by the engulfed particles (39). Moreover, microfluorimetric assay revealed that cellular uptake of nanoparticles was rapid (onset, 5 min) and high (120 µg nanoparticles per milligram cell protein). Cellular uptake by endocytosis was previously reported as the internalization mechanism for chitosan (33, 34,57) and other particles in the colloidal range (58–60). Endocytic uptake was energy-dependent; this would explain the low uptake values (12 µg/mg) at 4°C. Our findings corroborated those previously demonstrating that energy-dependent endocytic processes account for up to 85% of the cellular uptake of chitosan nanoparticles (34,61). Our mechanistic studies revealed that endocytic uptake of CS nanoparticles showed a significant involvement of clathrin-mediated translocation (62).

In an early publication, CTX solution was reported to reduce the bacterial burden within the reticuloendothelial system, where salmonellae were thought to exist intracellularly (2). A more recent study (9) showed that CTX had no bactericidal effect on *S. typhimurium* in a mouse macrophage cell line. Pragmatically, the intracellular activity of antibiotics entrapped in nanoparticles was evaluated herein by adding the nanosystems to cells (enterocytes/phagocytes) pre-infected with *S. typhimurium* and counting the remaining intracellular microorganisms following exposure to external gentamicin solution to kill extracellular bacteria (63). The CTX–chitosan nanoparticles resulted in a significantly higher reduction in bacterial count in Caco-2 and macrophages J774.2 as compared with placebo nanoparticles, CTX, and CTX–chitosan solutions. These results suggest that dual mechanism might account for the enhanced antibacterial effect of CTX–CS nanoparticles: first, the endocytic uptake of appreciable amounts of CTX as nanoparticles and second, the antibacterial effect of chitosan. The CTX–CS nanoparticles formulation was extremely and significantly superior to both free CTX and CTX–CS solution in the bactericidal effect. This could be attributed to enhanced cellular uptake by adsorptive endocytosis and subsequent release of adsorbed/entrapped antibiotic. Endocytic uptake of particulate system provided access for drugs which otherwise are cell membrane-impermeative (23). This was reported for liposomal gentamicin formulations against intracellular *S. typhimurium* and *Listeria monocytogenes* (64). Targeting phagocytic cells/cytoplasmic delivery is justified through nanoparticle technology (27,29,65). The enhancement of antibacterial effect of CTX might be a consequence of chitosan acting as absorption enhancers for drugs (66–69); however, CTX–CS nanoparticles exerted a significantly higher antibacterial effect than CTX–CS solution (99% bacterial killing), indicating that the nanoparticulate system and not just the chitosan polymer is an asset. The endocytic pathway adopted by

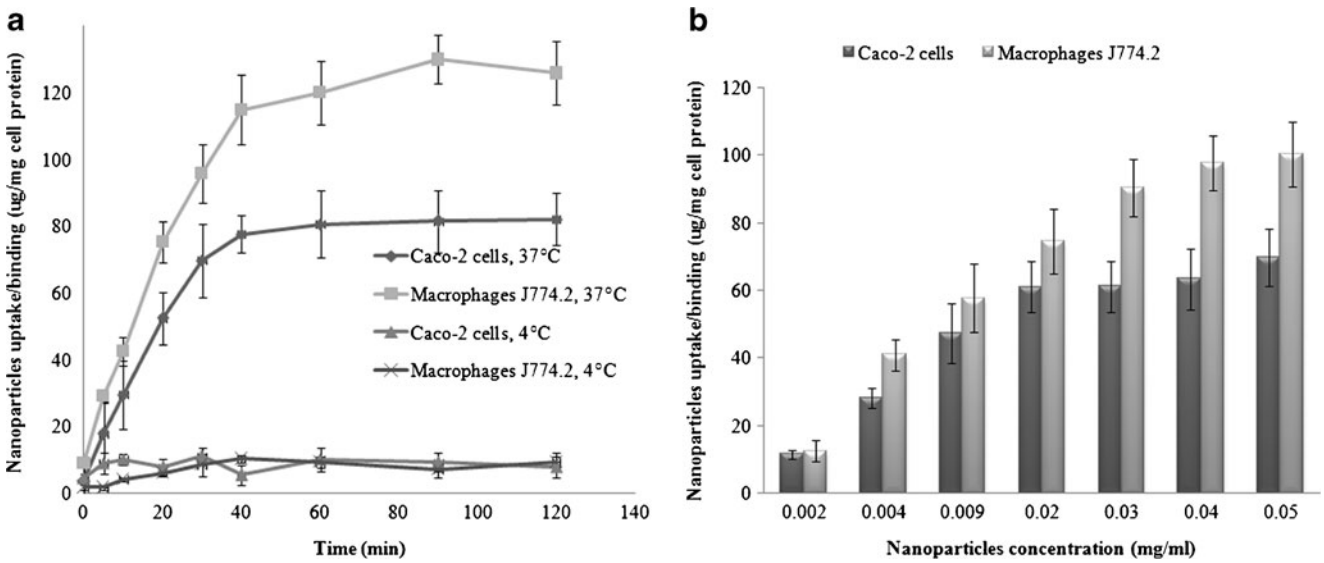

Fig. 4. Cellular uptake of nanoparticles as a function of **a** incubation time at nanoparticle dose of 0.02 mg/ml and **b** nanoparticles concentration 30 min post-incubation with Caco-2 and macrophages J774.2 cells at 37°C as measured by the microfluorimetry technique. The formula tested (CS, 1 mg/mL; TPP, 1 mg/mL at CS/TPP ratio=9:1 and pH 5/5)

CTX–CS nanoparticles could shuttle appreciable amounts of CTX to the intracellular milieu in contrast to the pinocytic process assumed by CTX solution alone or CTX solution with chitosan; the latter is not concentrative and depends only on the extracellular concentration of the drug (70). On the other hand, the finding that placebo (drug-free) CS nanoparticles exhibited a reduction in bacterial count suggests that the antibacterial (71–73) and antityphoid effect of chitosan against *S. typhimurium* and other Gram-negative bacteria (49,50) might also account for the augmented antibacterial effect of the CTX–CS nanoparticles. The ability of nanoparticles loaded with beta-lactam antibiotics to evade the efflux system needs be tested in future studies.

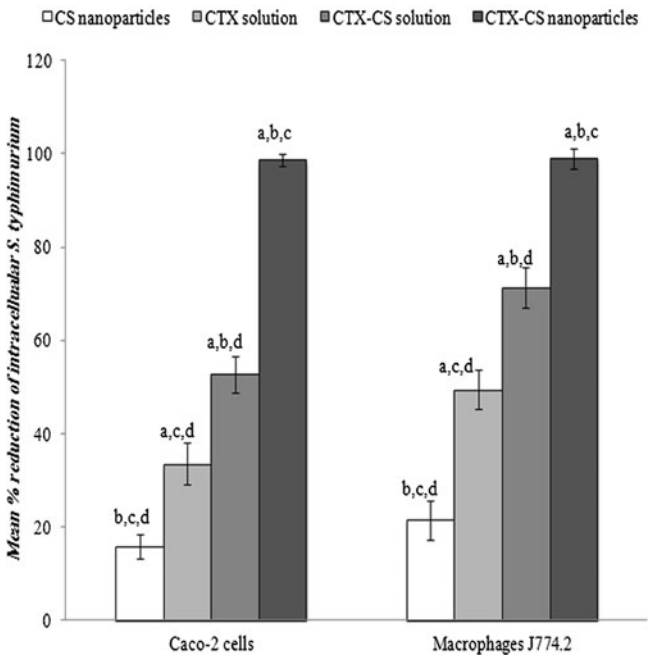

Fig. 5. Antibacterial activity of different CTX–CS nanoparticles in Caco-2 and macrophages J774.2 cell lines pre-infected with *S. typhimurium* and treated with gentamicin sulfate (200 $\mu g/ml^{-1}$ h) to kill extracellular bacteria. The nanoparticles formulation (CTX, 1 mg/ml; CS, 1 mg/mL; TPP, 1 mg/mL at CS/TPP ratio=9:1 and pH 5/5) was tested at a concentration of 0.12 mg/ml equivalent to 50 μg/ml CTX. **a**, **b**, **c**, or **d** Significantly different from CS nanoparticles, CTX solution, CTX–CS solution, or CTX–CS nanoparticles, respectively, at $P<0.05$ using one-way ANOVA followed by Bonferroni test for multiple comparison

CONCLUSION

Chitosan in properly designed nanosized formulations loaded with ceftriaxone has demonstrated potential as a safe delivery system for targeting *Salmonella*-infected cells. The nanoparticles were shown to be internalized by Caco-2 as well as by macrophages J774.2 with rapid cellular uptake kinetics. The antibacterial effect was significantly improved compared with CTX solution in both cell lines used. Chitosan biomaterial formulated as nanoparticles augmented the antibacterial effect of CTX against intracellular *S. typhimurium*. The enhanced intraphagocytic delivery of the third-generation cephalosporin member, traditionally thought to be non-internalized, seemed very promising for treatment of intracellular bacteria. Research is needed to proceed on other intracellularly residing pathogens *in vivo* as well as clinically.

ACKNOWLEDGMENTS

The authors are thankful to the bioimaging facility, Faculty of Life Sciences, University of Manchester, for assistance in confocal microscopy studies. The authors are also grateful to Prof. Nicola Tirelli, University of Manchester, for supporting the preliminary work.

REFERENCES

1. Eickhoff TC, Ehret J. Comparative *in vitro* studies of Ro 13-9904, a new cephalosporin derivative. Antimicrob Agents Chemother. 1981;19(3):435–42.
2. Anton PA, Kemp JA, Butler T, Jacobs MR. Comparative efficacies of ceftriaxone, moxalactam, and ampicillin in experimental *Salmonella typhimurium* infection. Antimicrob Agents Chemother. 1982;22(2):312–5.
3. Keenholtz SL, Jacobus NV, Tally FP, Gorbach SL. *In vitro* activity of ceftazidime and ceftriaxone. Clin Ther. 1983;5(6):603–16.
4. Neu HC, Meropol NJ, Fu KP. Antibacterial activity of ceftriaxone (Ro 13-9904), a beta-lactamase-stable cephalosporin. Antimicrob Agents Chemother. 1981;19(3):414–23.
5. Kuhn H, Angehrn P, Havas L. Autoradiographic evidence for penetration of 3H-ceftriaxone (Rocephin) into cells of spleen, liver and kidney of mice. Chemotherapy. 1986;32(2):102–12.
6. Beskid G, Christenson JG, Cleeland R, DeLorenzo W, Trown PW. *In vivo* activity of ceftriaxone (Ro 13-9904), a new broad-spectrum semisynthetic cephalosporin. Antimicrob Agents Chemother. 1981;20(2):159–67.
7. Lemaitre BC, Mazigh DA, Scavizzi MR. Failure of beta-lactam antibiotics and marked efficacy of fluoroquinolones in treatment of murine *Yersinia* pseudotuberculosis infection. Antimicrob Agents Chemother. 1991;35(9):1785–90.
8. Maurin M, Mersali NF, Raoult D. Bactericidal activities of antibiotics against intracellular *Francisella tularensis*. Antimicrob Agents Chemother. 2000;44(12):3428–31.
9. Chiu CH, Lin TY, Ou JT. *In vitro* evaluation of intracellular activity of antibiotics against non-typhoid *Salmonella*. Int J Antimicrob Agents. 1999;12(1):47–52.
10. Moulin F, Sauve-Martin H, Marc E, Lorrot M, Soulier M, Ravilly S, *et al*. Ciprofloxacin after clinical failure of ceftriaxone for severe salmonellosis in children. Internet J Infect Dis. 2003;3.
11. Lipinski CA, Lombardo F, Dominy BW, Feeney PJ. Experimental and computational approaches to estimate solubility and permeability in drug discovery and development settings. Adv Drug Deliv Rev. 2001;46(1–3):3–26.
12. Lee S, Kim SK, Lee DY, Chae SY, Byun Y. Pharmacokinetics of a new, orally available ceftriaxone formulation in physical complexation with a cationic analogue of bile acid in rats. Antimicrob Agents Chemother. 2006;50(5):1869–71.
13. Mrestani Y, Mrestani-Klaus C, Bretschneider B, Neubert RH. Improvement of lipophilicity and membrane transport of cefuroxime using *in vitro* models. Eur J Pharm Biopharm. 2004;58(3):653–7.
14. Mrestani Y, Hartl A, Neubert RH. Influence of absorption enhancers on the pharmacokinetic properties of non-oral beta-lactam-cefpirom using the rabbit (*Chinchilla*) *in vivo* model. Int J Pharm. 2006;309(1–2):67–70.
15. Mrestani Y, Bretschneider B, Hartl A, Neubert RH. *In-vitro* and *in-vivo* studies of cefpirom using bile salts as absorption enhancers. J Pharm Pharmacol. 2003;55(12):1601–6.
16. Mrestani Y, Bretschneider B, Hartl A, Brandsch M, Neubert RH. Influence of enhancers on the absorption and on the pharmacokinetics of cefodizime using *in-vitro* and *in-vivo* models. J Pharm Pharmacol. 2004;56(4):485–93.
17. Lee S, Kim SK, Lee DY, Park K, Kumar TS, Chae SY, *et al*. Cationic analog of deoxycholate as an oral delivery carrier for ceftriaxone. J Pharm Sci. 2005;94(11):2541–8.
18. Cho SW, Lee JS, Choi SH. Enhanced oral bioavailability of poorly absorbed drugs. I. Screening of absorption carrier for the ceftriaxone complex. J Pharm Sci. 2004;93(3):612–20.
19. Briones E, Colino CI, Lanao JM. Delivery systems to increase the selectivity of antibiotics in phagocytic cells. J Control Release. 2008;125(3):210–27.
20. Nacucchio MC, Di Rocco PH, Sordelli DO. Liposomes as carriers for antibiotics. Targeted Diagn Ther. 1990;3:337–54.
21. Zhang Q, Liao GT, Wei DP, Zhang CJ. Increase of gentamicin uptake in cultured mouse peritoneal macrophage and rat hepatocytes when used in the form of nanoparticles. Yao Xue Xue Bao. 1996;31(5):375–80.
22. Bakker-Woudenberg IA. Delivery of antimicrobials to infected tissue macrophages. Adv Drug Deliv Rev. 1995;17:5–20.
23. Couvreur P, Fattal E, Andremont A. Liposomes and nanoparticles in the treatment of intracellular bacterial infections. Pharm Res. 1991;8(9):1079–86.
24. Gamazo C, Prior S, Concepcion Lecaroz M, Vitas AI, Campanero MA, Perez G, *et al*. Biodegradable gentamicin delivery systems for parenteral use for the treatment of intracellular bacterial infections. Expert Opin Drug Deliv. 2007;4(6):677–88.
25. Lecaroz MC, Blanco-Prieto MJ, Campanero MA, Salman H, Gamazo C. Poly(D, L-lactide-coglycolide) particles containing gentamicin: pharmacokinetics and pharmacodynamics in *Brucella melitensis*-infected mice. Antimicrob Agents Chemother. 2007;51(4):1185–90.
26. Balland O, Pinto-Alphandary H, Viron A, Puvion E, Andremont A, Couvreur P. Intracellular distribution of ampicillin in murine macrophages infected with *Salmonella typhimurium* and treated with (3H)ampicillin-loaded nanoparticles. J Antimicrob Chemother. 1996;37(1):105–15.
27. Gaspar MM, Cruz A, Fraga AG, Castro AG, Cruz ME, Pedrosa J. Developments on drug delivery systems for the treatment of mycobacterial infections. Curr Top Med Chem. 2008;8(7):579–91.
28. Lecaroz C, Gamazo C, Blanco-Prieto MJ. Nanocarriers with gentamicin to treat intracellular pathogens. J Nanosci Nanotechnol. 2006;6(9–10):3296–302.
29. Torchilin VP. Multifunctional nanocarriers. Adv Drug Deliv Rev. 2006;58(14):1532–55.
30. Lecaroz C, Blanco-Prieto MJ, Burrell MA, Gamazo C. Intracellular killing of *Brucella melitensis* in human macrophages with microsphere-encapsulated gentamicin. J Antimicrob Chemother. 2006;58(3):549–56.
31. Lecaroz C, Gamazo C, Renedo MJ, Blanco-Prieto MJ. Biodegradable micro- and nanoparticles as long-term delivery vehicles for gentamicin. J Microencapsul. 2006;23(7):782–92.
32. Lu E, Franzblau S, Onyuksel HCP. Preparation of aminoglycoside-loaded chitosan nanoparticles using dextran sulphate as a counterion. J Microencapsul. 2009;26(4):346–54.
33. Huang M, Khor E, Lim LY. Uptake and cytotoxicity of chitosan molecules and nanoparticles: effects of molecular weight and degree of deacetylation. Pharm Res. 2004;21(2):344–53.
34. Huang M, Ma Z, Khor E, Lim LY. Uptake of FITC-chitosan nanoparticles by A549 cells. Pharm Res. 2002;19(10):1488–94.
35. Calvo P, Remunan-Lopez C, Vila-Jato JL, Alonso MJ. Chitosan and chitosan/ethylene oxide-propylene oxide block copolymer nanoparticles as novel carriers for proteins and vaccines. Pharm Res. 1997;14(10):1431–6.
36. Gan Q, Wang T, Cochrane C, McCarron P. Modulation of surface charge, particle size and morphological properties of chitosan-TPP nanoparticles intended for gene delivery. Colloids Surf B Biointerfaces. 2005;44(2–3):65–73.
37. Zheng Y, Yang W, Wang C, Hu J, Fu S, Dong L, *et al*. Nanoparticles based on the complex of chitosan and polyaspartic acid sodium salt: preparation, characterization and the use for 5-fluorouracil delivery. Eur J Pharm Biopharm. 2007;67(3):621–31.
38. Zaki NM, Mortada ND, Awad GA, Abd ElHady SS. Rapid-onset intranasal delivery of metoclopramide hydrochloride part II: safety of various absorption enhancers and pharmacokinetic evaluation. Int J Pharm. 2006;327(1–2):97–103.
39. Zaki NM, Tirelli N. Assessment of nanomaterials cytotoxicity and internalization. Methods Mol Biol. 2011;695:243–59.
40. Mosmann T. Rapid colorimetric assay for cellular growth and survival: application to proliferation and cytotoxicity assays. J Immunol Methods. 1983;65(1–2):55–63.
41. Fischer D, Li Y, Ahlemeyer B, Krieglstein J, Kissel T. *In vitro* cytotoxicity testing of polycations: influence of polymer structure on cell viability and hemolysis. Biomaterials. 2003;24(7):1121–31.
42. Zhang Z, Huey Lee S, Feng SS. Folate-decorated poly(lactide-co-glycolide)-vitamin E TPGS nanoparticles for targeted drug delivery. Biomaterials. 2007;28(10):1889–99.
43. Tang P, Foubister V, Pucciarelli MG, Finlay BB. Methods to study bacterial invasion. J Microbiol Methods. 1993;18:227–40.
44. Bretschneider B, Brandsch M, Neubert R. Intestinal transport of beta-lactam antibiotics: analysis of the affinity at the H+/peptide

symporter (PEPT1), the uptake into Caco-2 cell monolayers and the transepithelial flux. Pharm Res. 1999;16(1):55–61.
45. Saitoh H, Gerard C, Aungst BJ. The secretory intestinal transport of some beta-lactam antibiotics and anionic compounds: a mechanism contributing to poor oral absorption. J Pharmacol Exp Ther. 1996;278(1):205–11.
46. Saitoh H, Fujisaki H, Aungst BJ, Miyazaki K. Restricted intestinal absorption of some beta-lactam antibiotics by an energy-dependent efflux system in rat intestine. Pharm Res. 1997;14(5):645–9.
47. Saitoh H, Aungst BJ, Tohyama M, Hatakeyama Y, Ohwada K, Kobayashi M, *et al*. *In vitro* permeation of beta-lactam antibiotics across rat jejunum and its correlation with oral bioavailability in humans. Br J Clin Pharmacol. 2002;54(4):445–8.
48. Nasti A, Zaki NM, de Leonardis P, Ungphaiboon S, Sansongsak P, Rimoli MG, *et al*. Chitosan/TPP and chitosan/TPP-hyaluronic acid nanoparticles: systematic optimisation of the preparative process and preliminary biological evaluation. Pharm Res. 2009;26(8):1918–30.
49. Yadav AV, Bhise SB. Chitosan: a potential biomaterial effective against typhoid current science. Curr Sci 2004;87(9):1176–1178.
50. Rabea EI, Badawy ME, Stevens CV, Smagghe G, Steurbaut W. Chitosan as antimicrobial agent: applications and mode of action. Biomacromolecules. 2003;4:1457–65.
51. Wu Y, Yang W, Wang C, Hu J, Fu S. Chitosan nanoparticles as a novel delivery system for ammonium glycyrrhizinate. Int J Pharm. 2005;295(1–2):235–45.
52. Oyarzun-Ampuero FA, Brea J, Loza MI, Torres D, Alonso MJ. Chitosan-hyaluronic acid nanoparticles loaded with heparin for the treatment of asthma. Int J Pharm 2009;381:122-129.
53. MacLaughlin FC, Mumper RJ, Wang J, Tagliaferri JM, Gill I, Hinchcliffe M, *et al*. Chitosan and depolymerized chitosan oligomers as condensing carriers for *in vivo* plasmid delivery. J Control Release. 1998;56(1–3):259–72.
54. Zhang DY, Shen XZ, Wang JY, Dong L, Zheng YL, Wu LL. Preparation of chitosan-polyaspartic acid-5-fluorouracil nanoparticles and its anti-carcinoma effect on tumor growth in nude mice. World J Gastroenterol. 2008;14(22):3554–62.
55. Gan Q, Wang T. Chitosan nanoparticle as protein delivery carrier—systematic examination of fabrication conditions for efficient loading and release. Colloids Surf B Biointerfaces. 2007;59(1):24–34.
56. Kean T, Roth S, Thanou M. Trimethylated chitosans as non-viral gene delivery vectors: cytotoxicity and transfection efficiency. J Control Release. 2005;103(3):643–53.
57. Harush-Frenkel O, Debotton N, Benita S, Altschuler Y. Targeting of nanoparticles to the clathrin-mediated endocytic pathway. Biochem Biophys Res Commun. 2007;353(1):26–32.
58. Vasir JK, Labhasetwar V. Biodegradable nanoparticles for cytosolic delivery of therapeutics. Adv Drug Deliv Rev. 2007;59(8):718–28.
59. Yuan H, Miao J, Du Y-Z, You J, Hu F-Q, Zeng S. Cellular uptake of solid lipid nanoparticles and cytotoxicity of encapsulated paclitaxel in A549 cancer cells. Int J Pharm. 2008;348(1–2):137–45.
60. Coester C, Nayyar P, Samuel J. *In vitro* uptake of gelatin nanoparticles by murine dendritic cells and their intracellular localisation. Eur J Pharm Biopharm. 2006;62(3):306–14.
61. de Enriquez Salamanca A, Diebold Y, Calonge M, Garcia-Vazquez C, Callejo S, Vila A, *et al*. Chitosan nanoparticles as a potential drug delivery system for the ocular surface: toxicity, uptake mechanism and *in vivo* tolerance. Invest Ophthalmol Vis Sci. 2006;47(4):1416–25.
62. Zaki NM, Nasti A, Tirelli N. Nano-carriers for cytoplasmic delivery: cellular uptake and intracellular fate of chitosan and hyaluronic acid-coated chitosan nanoparticles in a phagocytic cell model. Macromol Biosci. 2011;11:1747–60.
63. Van den Broek PJ. Activity of antibiotics against microorganisms ingested by mononuclear phagocytes. Eur J Clin Microb Infect Dis. 1991;10:114–8.
64. Lutwyche P, Cordeiro C, Wiseman DJ, St-Louis M, Uh M, Hope MJ, *et al*. Intracellular delivery and antibacterial activity of gentamicin encapsulated in pH-sensitive liposomes. Antimicrob Agents Chemother. 1998;42(10):2511–20.
65. Panyam J, Labhasetwar V. Targeting intracellular targets. Curr Drug Deliv. 2004;1(3):235–47.
66. Davis SS, Illum L. Absorption enhancers for nasal drug delivery. Clin Pharmacokinet. 2003;42(13):1107–28.
67. Di Colo G, Burgalassi S, Zambito Y, Monti D, Chetoni P. Effects of different *N*-trimethyl chitosans on *in vitro*/*in vivo* ofloxacin transcorneal permeation. J Pharm Sci. 2004;93 (11):2851–62.
68. Kowapradit J, Opanasopit P, Ngawhiranpat T, Apirakaramwong A, Rojanarata T, Ruktanonchai U, *et al*. Methylated *N*-(4-*N*, *N*-dimethylaminobenzyl) chitosan, a novel chitosan derivative, enhances paracellular permeability across intestinal epithelial cells (Caco-2). AAPS PharmSciTech. 2008;9(4):1143–52.
69. Mao S, Shuai X, Unger F, Simon M, Bi D, Kissel T. The depolymerization of chitosan: effects on physicochemical and biological properties. Int J Pharm. 2004;281(1–2):45–54.
70. Zaki NM, Tirelli N. Gateways for the intracellular access of nano-carriers: a review of receptor-mediated endocytosis mechanisms and of strategies in receptor targeting. Expert Opin Drug Deliv. 2010;7(8):895–913.
71. Sadeghi AM, Dorkoosh FA, Avadi MR, Saadat P, Rafiee-Tehrani M, Junginger HE. Preparation, characterization and antibacterial activities of chitosan, *N*-trimethyl chitosan (TMC) and *N*-diethylmethyl chitosan (DEMC) nanoparticles loaded with insulin using both the ionotropic gelation and polyelectrolyte complexation methods. Int J Pharm. 2008;355(1–2):299–306.
72. No HK, Park NY, Lee SH, Meyers SP. Antibacterial activity of chitosans and chitosan oligomers with different molecular weights. Int J Food Microbiol. 2002;74(1–2):65–72.
73. Raafat D, von Bargen K, Haas A, Sahl HG. Insights into the mode of action of chitosan as an antibacterial compound. Appl Environ Microbiol. 2008;74(12):3764–73.